© 2019. Published by The Company of Biologists Ltd | Journal of Experimental Biology (2019) 222, jeb209965. doi:10.1242/jeb.209965

RESEARCH ARTICLE

From injury to full repair: nerve regeneration and functional recovery in the common octopus, *Octopus vulgaris*

Pamela Imperadore[1,2,*], Dario Parazzoli[3], Amanda Oldani[3], Michael Duebbert[4], Ansgar Büschges[4] and Graziano Fiorito[2]

ABSTRACT

Spontaneous nerve regeneration in cephalopod molluscs occurs in a relative short time after injury, achieving functional recovery of lost capacity. In particular, transection of the pallial nerve in the common octopus (*Octopus vulgaris*) determines the loss and subsequent restoration of two functions fundamental for survival, i.e. breathing and skin patterning, the latter involved in communication between animals and concealment. The phenomena occurring after lesion have been investigated in a series of previous studies, but a complete analysis of the changes taking place at the level of the axons and the effects on the animals' appearance during the whole regenerative process is still missing. Our goal was to determine the course of events following injury, from impairment to full recovery. Through imaging of the traced damaged nerves, we were able to characterize the pathways followed by fibres during regeneration and end-target re-innervation, while electrophysiology and behavioural observations highlighted the regaining of functional connections between the central brain and periphery, using the contralateral nerve in the same animal as an internal control. The final architecture of a fully regenerated pallial nerve does not exactly mirror the original structure; however, functionality returns to match the phenotype of an intact octopus with no observable impact on the behaviour of the animal. Our findings provide new important scenarios for the study of regeneration in cephalopods and highlight the octopus pallial nerve as a valuable 'model' among invertebrates.

KEY WORDS: Nervous system, Pallial nerve, Stellate ganglion, Cephalopods, Multiphoton microscopy, Nerve backfilling

INTRODUCTION

More than 160 years of studies support evidence of outstanding regenerative abilities of cephalopod molluscs, showing that cuttlefish, squid and octopus are all capable of recovering the structure and function of a variety of damaged/lost tissues and parts, including the nervous system (reviewed in Imperadore and Fiorito, 2018). As in other organisms, the regenerative capabilities of cephalopods appear to rely on the plasticity expressed at the cellular level, and on the involvement of pluripotent elements such as stem cells or dedifferentiated cells, cell proliferation and migration (Imperadore et al., 2017, 2018; Zullo et al., 2017), and other regulatory and/or trophic factors including the expression of specific genes (for a general review, see Birnbaum and Alvarado, 2008; see also Imperadore, 2017).

One of the most remarkable cases of regeneration in cephalopods is represented by the pallial nerve, a paired neural structure connecting the central nervous system (i.e. the sub-oesophageal mass) to the periphery via the stellate ganglia (for description, see Fredericq, 1878; Young, 1929, 1971, 1972). These two long nerves, which extend around 40 mm in length in an adult octopus of about 250 g body mass having a mantle length of 95 mm, innervate mantle muscles and chromatophores in the skin (Fig. 1). Axons of neurons travelling in this nerve are involved in the neural control of respiratory muscles and skin patterning (Imperadore et al., 2017, 2018; Sanders and Young, 1974; Sereni, 1929; Sereni and Young, 1932).

Unilateral traumatic injury of this nerve leads to paralysis of mantle muscles and immediate paling of the skin on the ipsilateral side of the mantle (e.g. Imperadore et al., 2017; Sanders and Young, 1974). The ability of the pallial nerve to regenerate in octopus was discovered by Sereni and Young (1932), who described the phenomenon from a structural and morphological point of view. Subsequently, recovery of the chromatic function of the skin was also reported. In the course of the above-mentioned observations, it was shown that degeneration of both the central and peripheral stump of the pallial nerve occurred within the first 10 days after lesion, followed by an intense regeneration originating from the central stump first and later from the peripheral one (Imperadore et al., 2017; Sereni and Young, 1932; Young, 1972). Haemocyte infiltration was reported to occur for several days after nerve transection at the level of the cut stumps (Sereni and Young, 1932), together with active phagocytosis, scar formation and proliferation (Imperadore et al., 2017). Proliferation and, possibly, re-differentiation of connective tissue cells within the injured nerve were first observed by Imperadore and co-workers (2017, 2018).

The first signs of functional recovery of body patterning (i.e. chromatic and textural appearance of the skin; Borrelli et al., 2006; Messenger, 2001; for review, see Packard and Hochberg, 1977) have been reported to appear from 30 days post-lesion (Sanders and Young, 1974), but recent studies found that this may occur earlier, i.e. 7 days after injury (Imperadore et al., 2017).

Here, we integrated available knowledge on the morphological and physiological events occurring after severing the pallial nerve in *Octopus vulgaris*, by extending our previous observations beyond the first 14 days after injury (Imperadore et al., 2017), and report a new set of data describing the complete recovery of the nervous components and corresponding phenotypic appearance. Backfilling of the pallial nerve allowed detection of regenerating fibres in the nerve as early as 5 days to 5 months post-lesion. We assessed physiological recovery through examination of the conductivity of the axons in the pallial nerve at 5 months post-lesion. Furthermore,

[1]Association for Cephalopod Research - CephRes, 80133 Napoli, Italy. [2]Department of Biology and Evolution of Marine Organisms, Stazione Zoologica Anton Dohrn, 80121 Napoli, Italy. [3]IFOM-FIRC Institute of Molecular Oncology, via Adamello 16, 20139 Milan, Italy. [4]Institute for Zoology, Biocenter Cologne, University of Cologne, 50674 Cologne, Germany.

*Author for correspondence (p_imperadore@cephalopodresearch.org)

P.I., 0000-0002-9947-0971

Received 4 July 2019; Accepted 11 September 2019

Journal of Experimental Biology (2019) 222, jeb209965. doi:10.1242/jeb.209965

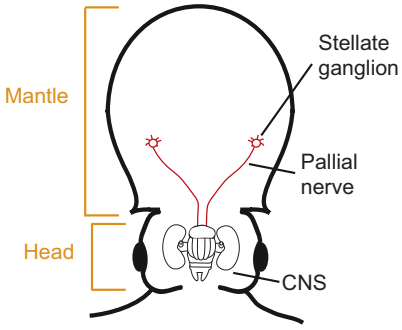

Fig. 1. Schematic overview of *Octopus vulgaris* anatomy. The centralized brain of the octopus (CNS) is positioned in the head of the animal, just between the two eyes. From the sub-oesophageal mass, on the ventral side of the CNS, two pallial nerves depart and innervate two stellate ganglia in the mantle. Each nerve and ganglion controls chromatophores (i.e. skin pattern) and mantle muscle (i.e. breathing) on the ipsilateral side of the mantle.

we provide a phenomenological analysis of mantle muscle contraction for breathing and chromatic patterning of the skin from loss of function (after lesion) to full recovery (~1–5 months post-lesion).

MATERIALS AND METHODS

Animals

A total of 14 *Octopus vulgaris* Cuvier 1797 of both sexes (8 females, 6 males, body mass 200–450 g) were utilized in this study. Animals were caught in the Bay of Naples (Italy) and following the practice available in G.F.'s laboratory at the Stazione Zoologica, Naples, Italy (Amodio et al., 2014; Fiorito et al., 1990), each animal was identified, sexed, weighed and housed in an experimental tank with running seawater. Octopuses were selected for being intact (i.e. no sign of lesion or regenerating parts).

Animal care and laboratory setting

Experiments were conducted during spring and autumn (seawater temperature ranging between 18 and 22°C). Following Fiorito and co-workers, the experimental setting was designed in order to simulate natural conditions at 3–4 m depth (Amodio et al., 2014; Borrelli, 2007; Fiorito and Scotto, 1992; Fiorito et al., 1990). Animals were individually housed in tanks located in a holding room with dark walls to which access was possible for experimenters and carers only. The tanks (60×100×50 cm) are made of dark grey PVC except for the front side, which consisted of a transparent glass panel (45×35 cm) to allow remote observation and video recording. A yellowish-brown layer of sand (355–500 µm granular size, 1 cm layer thickness), obtained directly from the coast off La Gaiola-Posillipo (Bay of Naples, Tyrrhenian Sea), was added to the bottom of each tank and a pair of bricks, set in a corner, served as a den. At the top of the tanks, a series of lamps (Neodymlite, Oy Airam AB, Finland) were positioned and programmed to switch on and off automatically according to the seasonal and daily rhythm at the latitude of the Bay of Naples. A dark blue curtain, from ceiling to the floor and running the entire length of the tanks, was positioned at a distance of 1.5 m from the front glass panel of each tank to hide both video equipment (video cameras, tripods, etc.) and the experimenter from the animals' view. A second curtain was positioned from the ceiling to the surface of the water at the level of the front glass panel. These curtains had a similar brightness to the tank walls, and also helped to hide the tester during the experiments.

Only animals fully capable of a normal predatory response (*sensu* Fiorito et al., 2015; Maldonado, 1963b) following acclimatization (about 1 week from capture; e.g. Fiorito et al., 1990; Maldonado, 1963a,b) were considered in this study.

Animals were presented with a live crab (*Carcinus maenas*) once a day to measure motivation to attack live prey – the so-called 'readiness to attack' (Amodio et al., 2014; see 'Analysis of animal performance', below, for details) – and as a food item.

Experiments with live octopuses included in this study were carried out before transposition of Directive 2010/63/EU in Italy (i.e. March 2014). Although no authorization was required, all procedures were performed in order to minimize the pain and distress of the animals involved (Andrews et al., 2013; Fiorito et al., 2014, 2015; Smith et al., 2013).

Nerve transection

Octopus vulgaris were anaesthetized by immersion in 3.5% magnesium chloride hexahydrate ($MgCl_2 \cdot 6H_2O$) in seawater for 15 min (Grimaldi et al., 2007). Surgery was performed as described in Imperadore et al. (2017). Briefly, octopuses were turned on their ventral side and the right pallial nerve exposed using a skin hooklet and completely transected using fine scissors. To standardize the site of injury along the nerve, the diameter of the stellate ganglion was measured for each animal. The same length was computed as the distance along the nerve to set the site of the lesion (3.5 mm on average). The completeness of the transection was verified under a stereo-microscope, allowing us to identify the two nerve stumps, which appeared with a gap in between of about 0.2 cm. The lesion did not require sutures. The left-side pallial nerve remained intact, serving as an internal control.

Animals were returned to their tanks soon after surgery and allowed to recover. Experiments were carried out only on animals that succeeded in recovering their predatory behaviour and that exhibited a stable and prompt attack behaviour in response to the live prey (Amodio et al., 2014; see 'Analysis of animal performance', below, for details).

Care of octopuses after surgery and during experimental observations

After recovery, octopuses were maintained in experimental tanks and kept alive for 5 days (N=3), 30 days (N=3), 45 days (N=3) and 5 months (N=5). Animals were observed daily to identify functional recovery for skin patterning, papillae and mantle muscle contraction. Animal care was provided on the basis of the established practice in G.F.'s laboratory (Stazione Zoologica, Naples, Italy) and in compliance with principles stated in Directive 2010/63/EU and guidelines available for the care and welfare of live cephalopods (Fiorito et al., 2014, 2015). All experiments were video recorded by remote-controlled cameras (Panasonic HDC-SD80 or Canon EOS 80D), which were hidden from the animals' view (Borrelli, 2007; Fiorito and Scotto, 1992; see above and Fiorito et al., 1990; Imperadore et al., 2017).

A live prey was presented to the octopus for a maximum of 5 min every day to assess the predatory response (i.e. readiness to attack). A failure to attack within this time was classified as 'no attack' (Amodio et al., 2014; Fiorito et al., 1990; Maldonado, 1963a,b). All behavioural observations were carried out at the same time of day, in the afternoon.

Analysis of animal performance

Video recordings of all animals were examined by independent observers, blind to the experimental design. For the purpose of this work we considered the predatory performance, behavioural

Journal of Experimental Biology (2019) 222, jeb209965. doi:10.1242/jeb.209965

responses, breathing rate and welfare status of the octopuses, as described below.

Predatory performance

The predatory performance of the octopuses was assessed through qualitative and semi-quantitative variables (Amodio et al., 2014; Borrelli, 2007; following Borrelli et al., 2006) by measuring readiness to attack and asymmetries during locomotory–predatory responses (i.e. type of attack/approach). As a measure of readiness to attack, we considered latency of attack (LA) measured as the time (in seconds) elapsed from the first appearance of a crab at the water surface to just before the octopus pounced on the prey.

The type of attack that *O. vulgaris* perform is reported to depend on the initial position and orientation that the animal assumes when the prey/stimulus comes into its visual field. In most cases, animals use one eye only (monocular vision; Packard, 1963), i.e. the 'positive' eye. We assessed the orientation towards the prey (i.e. asymmetries, side of attack/approach, SA: left, right) during attack/approach responses of the octopus to the prey.

The above parameters were measured every day before and after lesion.

Behavioural responses

Changes in the appearance of chromatic and textural patterns between the lesioned and control sides were assessed. These were recorded daily when the animal was at rest (at least 10 min before) and after the presentation of the live prey in the octopus' tank to assess its readiness to attack. Through analysis of the video recordings, two independent observers scored the body pattering and the approximate areas of blanching of the skin (mantle and any other body part) according to descriptions provided elsewhere (Packard, 1991, 1995; Sanders and Young, 1974). Body patterning observed during the analysis of video recordings was also coded following Borrelli et al. (2006).

Breathing rate

We assessed breathing rate through analysis of the video recordings. We also scored any side-bias in the use of the mantle musculature in providing efficient breathing movements. Snapshots of selected frames, where the animal appeared motionless, showing both sides of the mantle opening to the camera, were saved. At least 40 frames (∼5 snapshots per second considered in the analysis) taken from video recordings of each trial were subsequently analysed through ImageJ (https://imagej.nih.gov/ij/) to measure, from each frame, octopus head width (in pixels, as a reference) and the extension of the maximum mantle opening (for each side, calculated in pixels). For the sake of the following analysis, measures of mantle openings were considered as the relative difference in the maximum extension observed during each breathing act of the mantle opening on both sides.

Welfare status

Behavioural observations also served as an assessment of animals according to the principles stated in Directive 2010/63/EU. Signs based on appearance, behaviour and physiology were monitored following those included in table 5 of Fiorito et al. (2015).

Humane killing of octopuses

At the selected time points (5, 30, 45 days and 5 months), octopuses were anaesthetized by immersion in a 3.5% solution of $MgCl_2$ in seawater. Animal behavioural responses were also observed and video recorded during anaesthesia; skin reactions to pinch on both sides of the mantle were assessed using grooved forceps (as described in Butler-Struben et al., 2018) in lesioned and control animals. When terminal anaesthesia was achieved (>30 min; Grimaldi et al., 2007), death was confirmed by transection of dorsal aorta, in compliance with recommendations included in Annex IV of Directive 2010/63/EU (see Andrews et al., 2013; Fiorito et al., 2015). After death, both nerves were harvested and used for backfilling experiments to evaluate nerve regeneration patterns and target re-innervation.

Electrophysiology

Only nerves from animals kept alive for 5 months post-lesion, prior to undergo backfilling, were used for electrophysiology experiments. Electrical stimulation of axons in the nerve was applied before the injury site with a stimulation electrode and recording of the induced activity was measured close to the stellate ganglion with a recording electrode. Analogous areas were selected for the contralateral control nerves.

The pallial nerve and the stellate ganglion of recovered and control sides of experimental animals were harvested and placed in a saline-filled dish. Bipolar hook electrodes (e.g. Büschges et al., 1992; Sauer et al., 1995) were placed at both ends of the pallial nerve and the electrodes were isolated from the surrounding saline by silicon paste (Baysilone, Fa. GE Bayer Silicones). For stimulation of axons at one electrode, rectangular current pulses of 0.2 ms duration and variable amplitude were used (generated by a Grass S48 stimulator via a Grass SIU5 isolation unit). The resulting compound spike of axons in the pallial nerve was recorded extracellularly with the second electrode. Signals were pre-amplified by an isolated low-noise preamplifier (model MA101, Electronics workshop, Institute for Zoology, University of Cologne). The signal was further amplified and high- and low-pass filtered (high-pass: 300 Hz; low-pass: 3 kHz) using a 4-channel amplifier/signal conditioner (model MA102, Electronics workshop, Institute for Zoology, University of Cologne). Signals from the stimulation and recording electrodes were digitized and recorded at a sampling rate of 12 kHz using a Micro-1401-3 analog-to-digital converter (Cambridge Electronic Design Ltd, Cambridge, UK) and Spike2 software (Cambridge Electronic Design). The threshold amplitude of the stimulus for eliciting a compound spike in the pallial nerve was set to 1.0× threshold (T) (Büschges et al., 1992; Hooper and Schmidt, 2017). The amplitudes for the stimuli were normalized to this threshold.

For evaluation of amplitudes of the compound action potentials induced by electrical stimulation of the pallial nerve, for each stimulation strength, the mean and standard deviation were calculated (considering five original compound action potentials per stimulus strength). Mean values of compound action potentials (lesioned and contralateral intact nerve) were also plotted versus stimulus strength.

Tissue sampling and backfilling

Pallial nerves together with stellate ganglia and surrounding tissues were harvested from animals after death for neural tracing experiments. The backfill protocol was performed following Imperadore et al. (2019). In brief, the far end of the pallial nerve was placed in a Vaseline pool filled with tracer solution (Neurobiotin, 5% in distilled water, Vector Laboratories SP-1120, ID RRID:AB_2313575) while the remaining tissue was immersed in seawater. The tracer was left to diffuse for around 24 h at 4°C.

After dye diffusion, the tissues were fixed in 4% paraformaldehyde (PFA) in seawater for 1 h 30 min at 4°C and then washed in 0.1 mol l^{-1} phosphate-buffered saline (PBS,

Journal of Experimental Biology (2019) 222, jeb209965. doi:10.1242/jeb.209965

pH 7.4). Dehydration was performed with an ascending ethanol series (20 min each), followed by a mix of ethanol 100% and methyl salicylate (1:1, 20 min) and by two changes of methyl salicylate (5 min each). Rehydration was achieved with a descending ethanol series (20 min each). The samples were treated with collagenase/dispase and hyaluronidase in 0.1 mol l^{-1} PBS for 30 min at 37°C on a shaker (final concentration of the enzymes was 1 mg ml^{-1}).

After washing in 0.1 mol l^{-1} PBS+1% Triton X-100 (PBS-TX), samples were placed for pre-incubation in 10% normal goat serum (NGS) in PBS-TX overnight at 4°C and the following day incubated with streptavidin conjugated to Cy3 (Jackson ImmunoResearch JI016-160-084, 1:200) in PBS-TX+10% NGS overnight at 4°C. Nuclei counterstain was performed with DAPI (14.3 µmol l^{-1}) in PBS-TX at room temperature (2 h).

Samples were washed in 0.1 mol l^{-1} PBS and dehydrated with an ascending ethanol series (20 min each). For clearing, samples were immersed in 100% ethanol and methyl salicylate (1:1) for 20 min and then in pure methyl salicylate until the preparation was fully transparent and clear (usually 15 min). For visualization under the microscope, the whole nerve and ganglion were embedded in methyl salicylate in a metal slide (2 or 3 mm thick) closed on both sides by cover slips.

Imaging of backfilled nerves

Samples were imaged on a Leica TCS SP8X laser scanning confocal microscope or a Leica DMi8 microscope using a 10× (zoom factor 0.40) or a 20× air objective (zoom factor 0.75). Tile Z-stack experiments of whole-mount tissues were performed on backfilled nerve and stellate ganglion, for both lesioned and control samples. The laser was set at 550 nm for neurobiotin detection, while DAPI was excited at 405 nm. Z-step size was set at 5 µm. Pixel format size was set at 1024×1024.

To visualize connective tissues in the samples, an upright multiphoton microscope was used (Leica SP8 MP). Laser Chameleon Vision II (Coherent) was tuned to 1050 nm for simultaneous excitation of SHG and neurobiotin; and 405 nm for excitation of DAPI. Two non-descanned HyD detectors were utilized to detect SHG signal (filter BP 525/50) and red signal (BP 585/40); one internal HyD was utilized for the DAPI objective. In this case, a 10× (zoom factor 0.40) air objective with a numerical aperture of 0.3 was utilized. Z-stacks were set at a step size of 10 µm.

Images were processed using Leica software LAS X or Fiji software.

Animals utilized for statistical analysis

Analyses of data on lateralization and latency of attack were carried out on a total of 68 *O. vulgaris*: *N*=34 (20 females, 14 males) before and after surgery ('injured'), and *N*=34 (21 females, 13 males) naive octopuses (before and after anaesthesia) that served as the control.

Of the 34 animals belonging to the injured group, only 14 individuals were the live animals utilized in this study. The behavioural data for the remaining 20 animals were deduced from laboratory records and video recordings from previous experiments (Imperadore et al., 2017, 2018). In addition, and in application of the 3Rs principle (www.nc3rs.org.uk/the-3rs), behavioural data for the control group (*N*=34) were deduced from previous data available for *O. vulgaris* held in G.F.'s lab (at the Stazione Zoologica, Naples, Italy, between 2010 and 2013). Based on log notes for the G.F. lab animals, octopuses were selected for the following characteristics: (i) absence of lesion of any kind; (ii) body mass (ranging between 250 and 450 g); (iii) water temperature of the holding tanks during experimentation (18–22°C); and (iv) because they underwent anaesthesia according to the same protocol as the injured group of animals included in this study.

Experimental design and statistical analysis

The number of octopuses used in this study was chosen in an attempt to both obtain a statistically representative group and implement the 3Rs strategy, reducing the number to a minimum. To further reduce the number of animals used, we obtained behavioural data from previous experiments, conducted in the same laboratory (at Stazione Zoologica, Naples, Italy) in comparable conditions (see 'Animals utilized for statistical analysis', above). Experiments, data and subsequent analyses were performed following recommendations on experimental design and analysis in laboratory animals (Festing and Altman, 2002) and, more specifically, guidelines for the care and welfare of cephalopods in research (Fiorito et al., 2015). Behavioural observations from video recordings and data analysis were performed by investigators blind to the experimental conditions. The experimental design was assessed through the NC3Rs Experimental Design Assistant (https://www.nc3rs.org.uk/experimental-design-assistant-eda), achieving power >0.90.

Statistical analyses were performed using SPSS software (SPSS Inc., released 2009, PASW Statistics for Windows, version 18.0, Chicago) to analyse (i) lateralization, (ii) latency of attack and (iii) recovery of the breathing function. Asymmetries (i.e. lateralization) and latencies of attack for the 68 octopuses taken into account were noted before anaesthesia/surgery and on the day following the procedures. Following Zar (1999) and Siegel and Castellan (1988), we applied McNemar's test to examine differences in the side animals' utilized during attack/approach (SA; within groups) for the two conditions (injured and control); comparisons between groups were tested using the chi-square test. Yates' correction for continuity was applied when necessary. Within- and between-groups comparisons on latency of attack data were tested through the Wilcoxon test and Mann–Whitney *U* test, respectively.

For analysis of the recovery of breathing function after nerve regeneration, we applied a Friedman ANOVA followed by Bonferroni correction. Wilcoxon matched-pairs signed-rank tests were used as *post hoc* procedure.

Whenever appropriate, Monte Carlo simulations were utilized to calculate exact probability (Monte Carlo exact module available in SPSS), providing asymptotic *P*, a Monte Carlo probability value (MCP) and a 95% confidence interval (CI) of the MCP.

Where box and whisker plots were utilized to plot data, we used the SPSS graphical output standards (i.e. boxes represent the interquartile range, 25th to 75th percentiles, bars within boxes indicate the median values, whiskers indicate the 10th and 90th percentiles, and outliers are marked). In all cases, statistical differences were considered significant at $P<0.05$.

RESULTS

Effect of pallial nerve lesion on octopus' behaviour

After severing the right pallial nerve and following recovery from anaesthesia, all *O. vulgaris* returned to their dens, behaved normally and did not exhibit any sign of distress. In some instances and immediately after recovery from anaesthesia, octopuses exhibited grooming behaviour (see description in Borrelli et al., 2006) close to the injured area and/or inside the mantle cavity (Fig. 2E) on the side of lesion. In most instances, grooming disappeared after a few hours.

All octopuses were presented with a live crab 60 min after recovery and promptly attacked it in less than 30 s, performing their normal predatory behaviour; on most occasions, a full attack response was observed (see descriptions in Borrelli et al., 2006;

Journal of Experimental Biology (2019) 222, jeb209965. doi:10.1242/jeb.209965

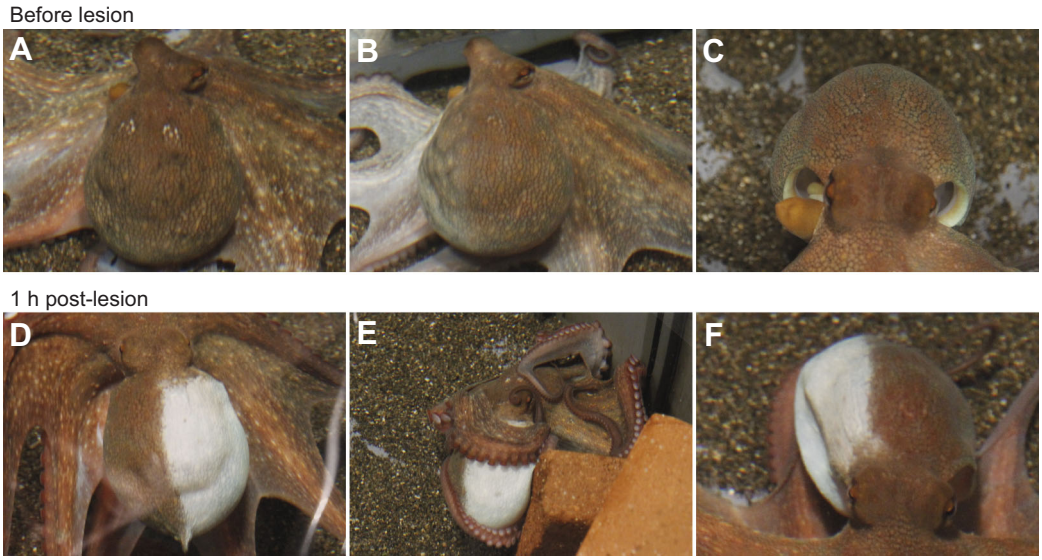

Fig. 2. Loss of function. Uninjured octopuses were able to perform the whole range of skin patterning on both sides of the mantle bilaterally (A) or controlling each side unilaterally (B). Normal breathing was detected on both sides of the mantle through expansion and contraction of mantle openings (C). After surgery (1 h post-lesion, p.l.), complete paling of the skin (D) and paralysis of respiratory muscles (F) was detected ipsilateral to the lesion. Grooming behaviour was observed in some of the injured animals soon after lesion (E).

Maldonado, 1963a,b; Packard, 1963). In order to evaluate any effect of the lesion, we considered the octopuses' predatory performance (median latency to attack before and after lesion, injured: LA_{before}=6.0 s, LA_{after}=5.9 s, P=0.966; control: LA_{before}=6.2 s, LA_{after}=6.9 s, P=0.993; after Wilcoxon signed-rank, N=34) and found no significant differences. We also compared predatory performance before and after anaesthesia or surgery in the two groups (injured LA_{before} versus control LA_{before}: Z=−0.343, P=0.731; injured LA_{after} versus control LA_{after}: Z=−0.527, P=0.598; both after Mann–Whitney U-test, N_1, N_2=34), confirming the two groups behaved similarly, independent of the treatment.

Furthermore, we considered the type of attack (i.e. SA: left or right) to assess whether the octopuses' behaviour was affected by treatment. Animals approached the prey consistently as they did before lesion (SA left versus right, injured: P=0.109; control: P=0.549; both after McNemar's test, N=34). Similarly, we tested the effect of SA between groups and found no significant difference (injured SA_{before} versus control SA_{before}: χ^2=0.23, P=0.627; injured SA_{after} and control SA_{after} χ^2=1.47, P=0.224; chi-squared test after Yates correction, N=68).

Loss of function and recovery

Before lesion, animals were fully able to exhibit their specific body pattern depending on the need, situation or stimulus they encountered in the tank and, in particular, to control bilaterally and unilaterally the chromatophores on each side of the mantle (Fig. 2A,B; see also Fig. S1A,B). However, immediately after recovery from surgery, half of the mantle (right side of the animal, i.e. the lesioned side) appeared white because of the absence of any chromatic and textural pattern (Fig. 2D). The contralateral side of the mantle retained the ability to perform the full range of body patterns, as in a normally behaving animal (Fig. 2D). We also observed paralysis of the mantle muscles on the lesioned side (compare Fig. 2C and Fig. 2F).

One to two days post-surgery, brown spots appeared on a pale background in the denervated area (see Fig. S1C) (see also Imperadore et al., 2017). At around the end of the first week/beginning of the second week post-surgery, injured octopuses exhibited some chromatic patterns on the lesioned side (see Fig. S1D), matching that on the contralateral uninjured side (at least in tone and grooves; see Fig. S1E). However, this capability was retained only when animals were at rest. Once moving around the tank and/or performing an attack/approach during the predatory response, immediate paling of the lesioned side was observed (see Fig. S1F). We did not notice further improvement at 2 weeks post-lesion. Full reappearance of the normal colour pattern of the skin occurred (injured *O. vulgaris* both at rest and during attack) after 45 days and in some cases 4 months after injury (see Fig. S1G,H; see also bottom right image in Fig. 3A). We observed recovery of the ability to control skin texture (linked to contraction and relaxation of papillae) from about 1 month after lesion (data not shown).

Pallial nerve transection also induced impairment of mantle contractions required by normal breathing (first week post-lesion; Fig. 3A, upper right image), when compared with both the contralateral mantle side and the same side before lesion (Fig. 3A, upper left image). We did not notice significant progress during the second week post-lesion, but improvement was observed between the third and fourth week post-lesion. Overall, we observed a significant departure from the baseline condition immediately after injury (Fig. 3B) and a recovery to the normal condition starting from the fifth week post-lesion. Efficient breathing on the lesioned side appeared restored only after about 1 month (between 37 and 45 days after surgery; Fig. 3A, lower left and right image, respectively).

We observed a trend in variation in the efficiency of breathing events after lesion (contraction/expansion of the mantle openings; χ^2=45.02, N=7, P<0.001, after Friedman ANOVA; Fig. 3B). The recovery continued to progress with time, with the difference between day 30 and day 37 post-lesion not being significant (day 30 versus day 37: Z=−0.68, N=7, P=0.499; Monte Carlo P<0.575, 95% CI=0.565–0.585, after Wilcoxon signed-rank test; Fig. 3B).

Wandering clouds on the denervated skin

We evaluated changes in appearance of the mantle skin at the end of the experiments once animals had been anaesthetized again for humane killing and tissue harvesting. At 5–8 min after immersion in

Journal of Experimental Biology (2019) 222, jeb209965. doi:10.1242/jeb.209965

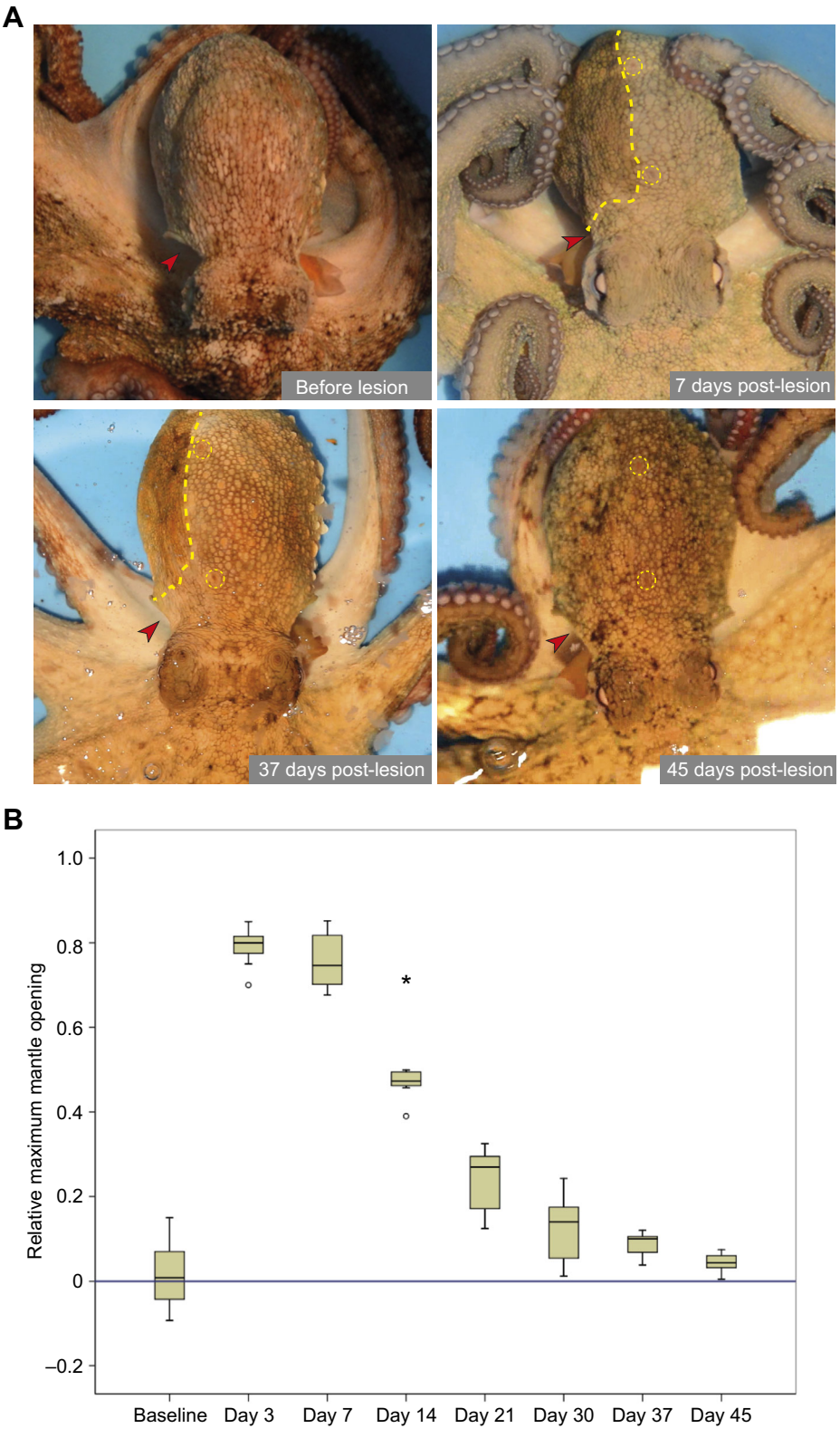

Fig. 3. Recovery of breathing function. (A) Pallial nerve transection interrupted the neural circuitry connecting the centralized brain to mantle muscles and chromatophores. The normal appearance of the animals (as shown in the upper left image) was disrupted. At 7 days post-lesion (upper right), the mantle muscles on the lesioned side (marked by red arrowheads in all the images in A) were visibly paralysed. The skin pattern on the same side of the mantle (highlighted by a yellow dashed line) was homogeneously coloured but greatly differed from that on the contralateral (uninjured) side and from the mantle of the animal before surgery. Restoration of breathing function was evident at 30–37 days post-lesion and was easily recognized by expansion and contraction of the mantle opening (red arrowhead, lower left image). No significant difference in muscle contraction was observed at 45 days post-lesion but an improved control of skin pattern was detected (lower right image). Main papillae (highlighted by yellow dashed circles) were used here as skin landmarks. (B) Box plot showing the relative difference in maximum extension of left (control) versus right (lesioned) side mantle openings of *O. vulgaris* during breathing acts before (baseline) and after lesion (*N*=14). A relative difference equal to zero (see reference line in the graph) is considered the normal condition. The plots show loss and recovery of breathing function with time (from day 3 to 45 post-lesion). Outliers are shown as circles and asterisks. Circles are for outliers with a value between 1.5 and 3 times the interquartile range (IQR); asterisks are for values greater than 3 times the IQR.

the anaesthetic solution, we observed that the right side of the mantle (injured octopuses: 5, 14 and 30 days post-lesion) appeared yellowish, while the contralateral side and the remaining part of the body were pale (see Fig. S2), as normally occurs following immersion in the $MgCl_2$ solution (Butler-Struben et al., 2018; Gleadall, 2013). When the dorsal part of the mantle was taken out of the anaesthetic solution, but leaving the other parts of the octopus body immersed, we observed dark waves (i.e. wandering clouds) on a grey-white background at the level of the denervated mantle (see Fig. S2).

The denervated skin was also highly sensitive to mechanical stimulation, contracting following pinching; the same stimulus did

not elicit any reaction on the contralateral side, as expected during anaesthesia (Butler-Struben et al., 2018; Gleadall, 2013).

This denervated skin area appeared to reduce in size with time. Indeed, using the four main papillae of the mantle as landmarks, we observed shrinkage of the area affected by these phenomena (i.e. wandering clouds, yellowing and mechanical excitability) a few days (around 5–7 days) post-lesion, as also described by Packard (1995), which continued to reduce with time. In particular, the skin along the midline, the mantle tip and close to the head on the injured side returned to its original appearance (see Fig. S2; see also Fig. 3A).

We observed the above-mentioned phenomena on the denervated skin during anaesthesia at all time points considered, until 30 days post-lesion (see Fig. S2). On occasion, when lesioned animals were anaesthetized 45 days post-lesion or later, the denervated side of the skin appeared as pale as the contralateral side (see Fig. S2), and wandering clouds were no longer observable. Under similar circumstances, skin contractions in response to light pinch or any mechanical stimulation were absent.

Regeneration of the pallial nerve

Backfilled contralateral control nerves did not show any differences in structure compared with naive control nerves (see Fig. S3 and Movie 1). Axons were traced from the nerve to the ganglion (see Fig. S3B,C); inside the ganglion, fibres grow around motoneurons and form the neuropil (see Fig. S3C left, and enlargement in the yellow rectangle). Some fibres were seen to exit through the stellar nerves, probably innervating chromatophores in the skin (see Fig. S3C). We also observed fibres originating from the centripetal cells of the stellate ganglion (see Fig. S3C right, Movie 1).

Lesion of the pallial nerve determined the formation of two stumps, a central one still connected to the brain (which was used for the tracing experiments) and a peripheral one, connected to the stellate ganglion in the periphery. Within the site of lesion and a few days post-surgery, a bridge of connective tissue appeared (see Fig. S4B,Bi). Fibres at 5 days post-lesion were not seen to cross the lesion site, but remained confined to the backfilled stump. When transected nerves were traced 30–45 days after surgery, axons were seen to cross the gap between the lesion and the ganglion (Fig. 4A,B; see also Movie 2). Even though axons appeared to regenerate in several directions, the majority of the tracked fibres found the right path, allowing them to enter the ganglion (Fig. 4A,B), where they formed a network around motoneurons (Fig. 4A,B,Biii). Furthermore, some of these axons were able to reach the stellate ganglion and also to leave it through the stellar nerves, probably to reach their final targets (i.e. chromatophores). At this time point (30–45 days post-lesion), no positive cells (i.e. centripetal cells) were ever observed inside the stellate ganglion, contrary to observations in naive and contralateral control ganglia (see Fig. S3C, Movie 1).

Regenerating fibres at the lesion site were moderately well organized in bundles, with each bundle able to direct toward the ganglion. Noteworthy, some of these axons were found close to the stellate ganglion, but did not make it through and were even seen to grow backwards and into the musculature (Fig. 4B,Bii).

The regenerated part of the growing axons did not appear to have a homogeneous calibre as in the case of intact fibres, but they showed multiple varicosities and some swelling. Branching and axon tip swelling were also observed for some of the axons that were not able to enter the ganglion (Fig. 4Bii).

At the level of the injury, regenerating fibres appeared to grow around non-fluorescent obstacles, possibly scar tissue or debris, which apparently diverted axons from a straight route (Fig. 4Bi; see also Movie 2).

Backfilling of pallial nerves at complete functional recovery showed a chaotic arrangement of fibres at the lesioned site, even though the majority of axons appeared to regenerate in the correct direction, i.e. towards the stellate ganglion (Fig. 5B, neurobiotin). We detected the presence of fibre thickenings (Fig. 5B), which were not observed at other time points or in the control nerves; varicosities and branching were still observable (Fig. 5D). Fibres were able to reach the ipsilateral stellate ganglion, form a network around motoneurons (Fig. 5C) and exit through the stellar nerves. Centripetal cells appeared, which traced back into the ganglion (Fig. 5C).

Tracing experiments also highlighted an increased number of vessels and small capillaries in lesioned nerves (Fig. 5B,D) again not visible in control nerves, suggesting the occurrence of angiogenesis during the regenerative events.

The site of lesion was recognizable as a tissue interruption (Fig. 5B, DAPI), being more evident on the dorsal side and less evident in the middle and ventral sides.

Functionality of regenerated axons in the pallial nerve

Regenerated fibres in the pallial nerve expressed axonal properties, as tested through two bipolar electrodes placed before the lesion site (central stump) and close to the stellate ganglion (peripheral stump) on the surgically isolated pallial nerve of regenerated animals 5 months post-lesion (Fig. 6A). Electrical stimulation via the stimulating electrode close to the central stump was found to systematically induce activity in axons crossing the lesion site in the recording electrodes close to the stellate ganglion in all experiments (Fig. 6B). With increasing stimulation amplitude, the extracellularly recorded compound action potential increased in two out of three preparations. Such an increase in compound action potential amplitude reveals that axons of different diameters are recruited upon stimulation of increasing strength (Fig. 6C). Interestingly, the activation of axons upon electrical stimulation in the contralateral control pallial nerve (Fig. 6A,C) showed a similar systematic correlation between stimulation strength and amplitude of the compound action potential.

DISCUSSION

Lesion of one of the two pallial nerves in *O. vulgaris* leads to the interruption of the neural circuits between the central brain and the stellate ganglion in the mantle (i.e. periphery). As each nerve and related ganglion controls only one side of the mantle (Fig. 1), loss of function can be immediately recognized on the ipsilateral side of the injury (see Fig. 2): this corresponds to skin paling (as originally observed by Fredericq, 1878) due to a lack of control of chromatophores in the skin and to the impairment of muscle function for the control of mantle breathing movements and papillae. The contralateral side preserves intact functionality (Imperadore et al., 2017). These dramatic changes appear reversible, because of the ability of the pallial nerve to functionally regenerate (Sanders and Young, 1974; Sereni and Young, 1932). We evaluated the timing and pathways of neural fibre regeneration and functional recovery for this nerve after complete transection.

All octopuses recovered the ability to control skin papillae at around 1 month following surgery. The first signs of mantle muscle contraction recovery, described as muscular tone improvement in Imperadore et al. (2017), were observed at 14 days post-lesion. Normal breathing was resumed between 30 and 37 days post-surgery for all individuals.

Journal of Experimental Biology (2019) 222, jeb209965. doi:10.1242/jeb.209965

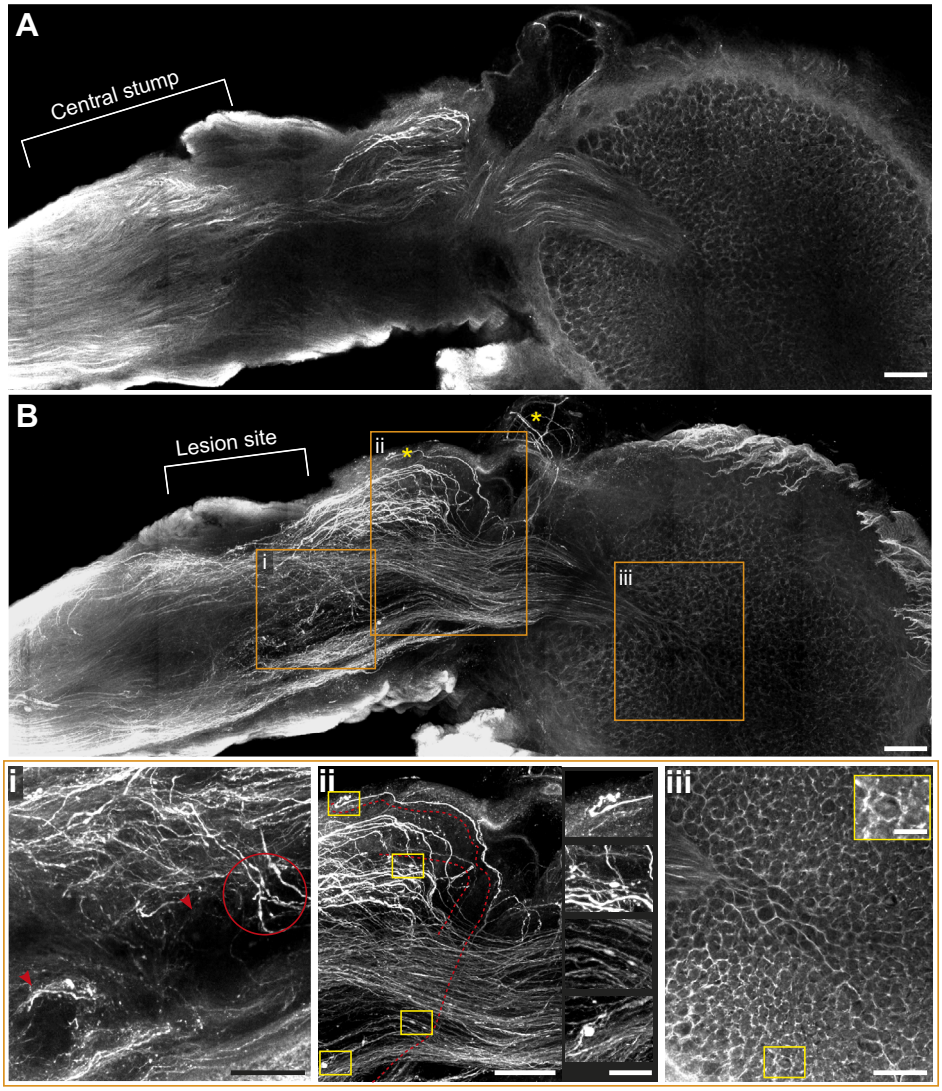

Fig. 4. Backfilling of the pallial nerve 45 days post-lesion. At 45 days after lesion, regenerating fibres bridged the gap between the two stumps, entering the stellate ganglion, where they formed a network among motoneurons (A,B). In A, it is possible to observe the central stump retaining a spike-like structure with fibres showing a homogeneous calibre and a straight direction. In B, proceeding deeper into the nerve in the area of the lesion, regenerating fibres appear to grow in several directions even though the majority of them are well organized and directed toward the stellate ganglion. Regenerating axons showed varicosities and variable calibre (red circle in Bi; yellow rectangles in Bii and corresponding enlargements on the right). In the original lesion site it was also possible to observe fibres growing around non-fluorescent obstacles (red arrowheads in Bi). Some fibres were also seen to deviate and grow into the musculature or backwards (red dotted lines in Bii). Tip swelling also occurred (top yellow rectangle in Bii and its enlargement to the right). Regenerating fibres were traced back into the stellate ganglion (Biii) where they formed a network around motoneurons (see enlarged area in the yellow rectangle in Biii). The image in B was obtained through maximum intensity projection of Z-stack images. The enlargements in Bi–iii correspond to the selected area of the original Z-stack, but with a reduced number of planes. Scale bars: 250 µm in A, B and Biii; 75 µm in Bi, Bii and enlargement in Biii.

These findings are also consistent with the morphological data obtained from imaging of the backfilled pallial nerves. Axons from the central stump required a comparable amount of time to reach motoneurons in the stellate ganglion (controlling breathing muscles; Monsell, 1977; Young, 1972), where they form a net surrounding them and possibly build synapses.

The time required by fibres to reach the chromatophores in the skin was consistently longer, as fibres had to reach the ganglion and exit from it through the stellar nerves, thus to travel for several centimetres to innervate the millions of chromatophores spread throughout the skin of the mantle (estimated at around 200 mm^{-2} in *O. vulgaris*: Messenger, 2001). All octopuses kept alive for 5 months after lesion were able to fully recover skin patterning. However, for one of them, 45 days was sufficient time, while two required around 2 months and the last two required 4 months for complete recovery. In all cases, animals anaesthetized for humane killing did not show wandering clouds on the skin of the lesioned side as observed at previous time points. The skin appeared as pale and as unreactive to pinch as the contralateral side of the mantle, comparable to what was observed in uninjured animals under anaesthesia.

If we consider regeneration and re-innervation in terms of fibre growth speed, we can speculate that axons from the central stump reach the stellate ganglion and completely re-establish synapsis with motoneurons at a speed of 10 µm h^{-1}, as they had to cover a distance of ∼3.5 mm to reach the ganglion and the same distance to pass through the ganglion. Our data confirm the rate of growth originally described by Sereni and Young (1932).

However, fibres directed from the nerve to the chromatophores apparently regenerate faster. Fibre speed in this case appears to be between approximatively 34 and 90 µm h^{-1}, considering 7 mm distance to exit the ganglion and around 90 mm to reach the farther chromatophores in the mantle, as is the case at complete recovery.

The large number of fibres found in the lesioned area together with their intricate pathways made it difficult to assess the true origin of the fibres. Even though we tracked axons from the central stump, we are not able to assert with certainty that these fibres originated from the central brain and not from the peripheral stump of the pallial nerve, which also start to regenerate a few days post-injury (Imperadore et al., 2017).

Fibre varicosities, swelling, branching, obstacle deviation and thickenings were visible in the regenerating nerves; the last of these were never observed in uninjured or contralateral nerves. Sereni and Young (1932) also report regenerating fibres deviating around obstacles; these may represent the residue of scars or debris of the degenerating materials, both identified a few days post-lesion

Journal of Experimental Biology (2019) 222, jeb209965. doi:10.1242/jeb.209965

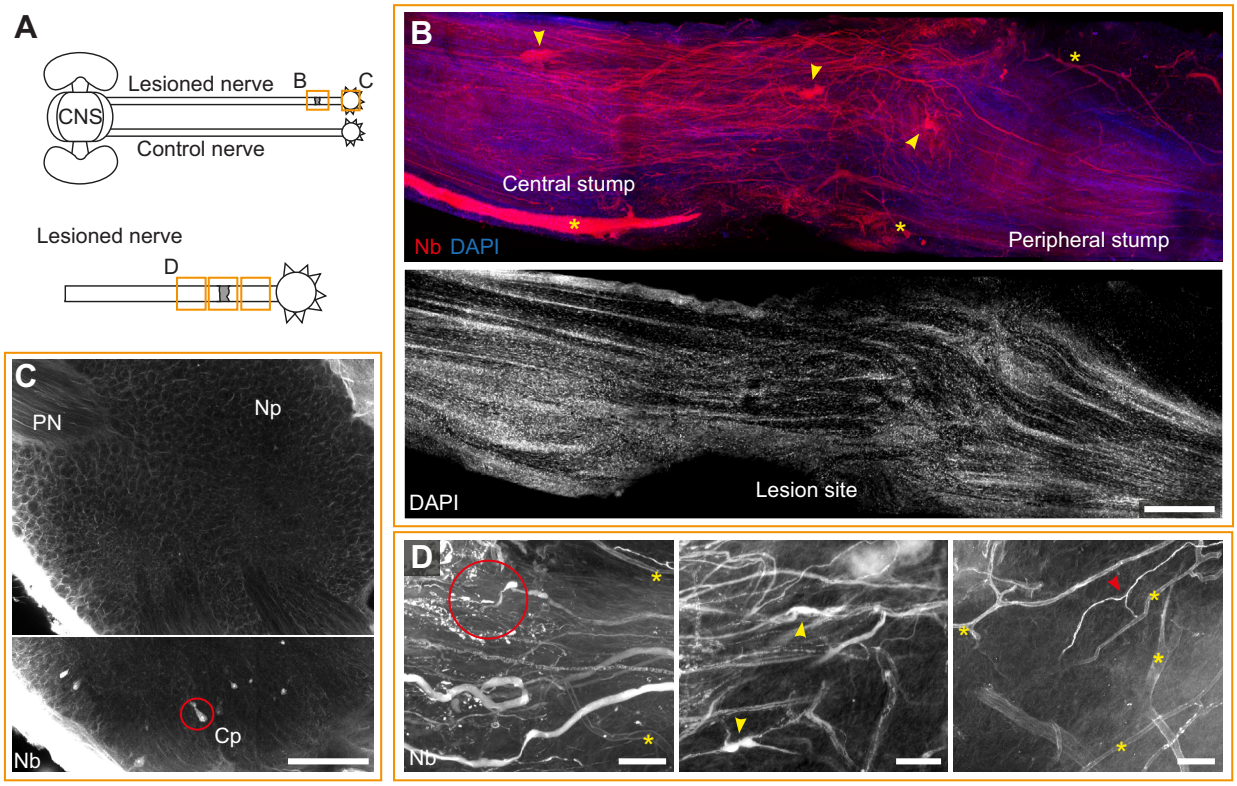

Fig. 5. Backfilling of the pallial nerve 5 months post-lesion. (A) Top, schematic drawing of the connections between the central brain (central nervous system, CNS) and the periphery through the pallial nerves (PN). The orange rectangles highlight areas corresponding to the lesioned pallial nerve and the ipsilateral stellate ganglion shown in the images in B and C, respectively. Bottom, schematic drawing of an enlargement of the lesioned pallial nerve and ipsilateral stellate ganglion. The orange rectangles highlight areas shown in the images in D. (B) An injured pallial nerve 5 months after surgery. Axons, traced through neurobiotin (Nb in red), were found to cross the site of the lesion, connecting the two stumps. While far from the injury, fibres retained the classic, well-ordered appearance, in the lesion site they appeared more chaotic, growing in several directions. Fibre thickenings of unknown function were visible in the nerve (yellow arrowheads). Neurobiotin also highlighted an increased number of vessels and small capillaries in the lesioned nerve (yellow asterisks). DAPI counterstain (blue in the merged image) allowed identification of the original site of transection, which appears as a tissue interruption. (D) Images corresponding to the three different areas in the bottom drawing in A, highlighting the presence of axon tip swelling and varicosities (red circle), thickenings (yellow arrowheads) and fibre branching (red arrowhead). An increased number of vessels and capillaries was visible in these areas (yellow asterisks). (C) Fibres from the regenerating nerve reach the ipsilateral stellate ganglion, form a network around motoneurons, and exit through the stellar nerves. Centripetal cells (Cp) were traced back into the ganglion (red circle). Np, neuropil. Scale bars: 500 µm in B and C; 75 µm in D.

(Imperadore et al., 2017, 2018) and also described to occur in mammals during peripheral nerve regeneration (Kang and Lichtman, 2013).

Swelling, branching and fibre aberration appear to persist for months; the regenerated nerves never regained their original appearance, even 5 months post-lesion, although all animals had perfectly recovered the normal function by this time.

We cannot exclude that alternative mechanisms might also be involved and aid in chromatophore re-innervation, such as intervention through collateral nerve sprouting of the stellar nerves from the opposite stellate ganglion (as suggested by Packard, 1995). This is further supported by the fact that the mantle midline and the areas close to it recover functionality much earlier than other areas (see Fig. S2). Further investigation is required to support this hypothesis.

Our electrophysiological experiments on samples taken 5 months post-lesion confirmed that lesioned nerves are able to re-establish functional connections between the brain and the periphery. The regenerated fibres express axonal properties, including voltage-dependent ion channels, and generate and propagate action potentials. Electrical stimulation via the stimulating electrode close to the central stump was found to systematically induce activity in axons crossing the lesion site in the recording electrodes close to the stellate ganglion. Increasing stimulation amplitude resulted in an increase in the extracellularly recorded compound action potential. Such an increase in compound action potential amplitude reveals that axons of different diameters are recruited upon stimulation of increasing strength (Büschges et al., 1992; Hooper and Schmidt, 2017).

Previous studies on regeneration of the pallial nerve in the octopus (Sanders and Young, 1974; Sereni and Young, 1932) considered 60–150 days for complete recovery of function of body patterning after injury (either through crush or cut). According to the authors, in some cases this never occurred and the animal continued to show a lack of full recovery (Sanders and Young, 1974; Sereni and Young, 1932). Complete recovery of body patterns after crushing the nerve required 9–10 weeks. However, no octopuses showed signs of colour pattern recovery until 50 days post-lesion, either in summer or in autumn when experiments were carried out (Sanders and Young, 1974; Sereni and Young, 1932). In the original study, six out of 10 animals recovered complete colour pattern (between 60 and 69 days), while only in two out of 10 octopuses was it possible to observe functional recovery of textural components (i.e. papillae; between 30 and 50 days). In contrast, only four animals

Journal of Experimental Biology (2019) 222, jeb209965. doi:10.1242/jeb.209965

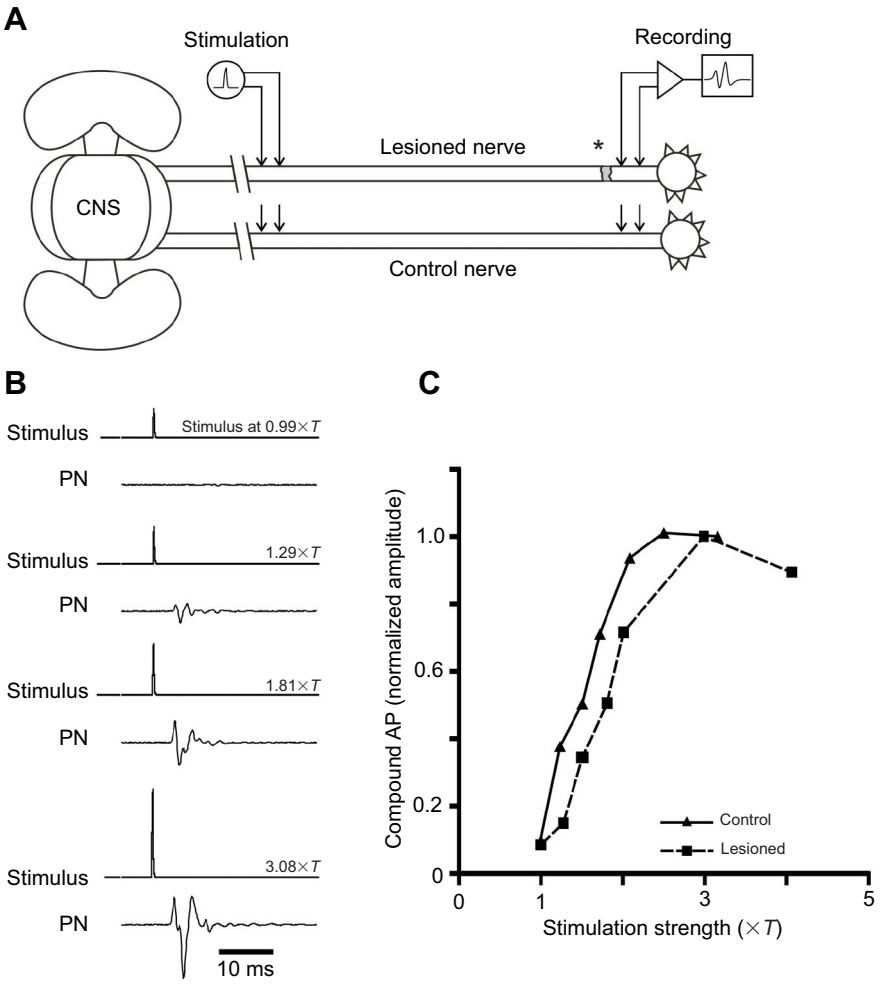

Fig. 6. Effect of electrophysiological stimulation of axons in the pallial nerve. (A) Schematic depiction of the stimulation setup. Bipolar extracellular electrodes were placed at two locations of the surgically isolated pallial nerve, which connects the brain and the stellate ganglion, for both the regenerated pallial nerve (top) and the control condition (bottom). The asterisk indicates the location of the lesion. (B) Effect of electrical stimulation on the regenerated pallial nerve (PN) at four stimulation intensities in one preparation: 0.99× threshold (i.e. below threshold, *T*) and 1.29, 1.81 and 3.08× threshold (i.e. above threshold). Note that the compound action potential increased with increasing stimulation amplitude (see Results). (C) Dependence of the normalized amplitude of the compound action potential (AP) induced by electrical stimulation in one regenerated nerve as compared with a control nerve. Data are means (*n*=5 stimulations each); standard deviation is not visible as the amplitude of the compound action potentials upon electrical stimulation only very slightly differed between trials for a given stimulation strength.

(out of 10) recovered colour patterns following complete transection of the pallial nerve (signs of recovery at 30 days). In this case, the complete regain of function required 109 days. In addition, seven out of 10 octopuses recovered the ability to raise papillae (Sanders and Young, 1974; Sereni and Young, 1932).

Strangely enough, when regenerated nerves were inspected, Young and co-workers were not able to determine any clear correlation between histological appearance and functional recovery, also noting the inability in following fibre pathways and orientations (Sanders and Young, 1974; Sereni and Young, 1932).

In summary, our results show that during pallial nerve regeneration, neural connectivity between the brain and the stellate ganglion can be re-established by the formation of axons crossing the lesion site.

In our view, the octopus pallial nerve provides an exceptional example of regeneration in cephalopods, because: (i) regeneration is always relatively quick and efficient; (ii) it is immediately possible to evaluate loss and regain of function by evaluating respiration (i.e. breathing movements) and skin patterning on the mantle of the animal; (iii) each animal has a pair of nerves, one on each side of the mantle, allowing the same animal to serve as both experiment and control; (iv) the same nerve can be lesioned several times, providing almost complete regeneration at each instance (Packard, 1995); and (v) the majority of the cell soma of axons in the pallial nerve reside inside the brain and the others reside in the ganglia at the periphery – both can regenerate, allowing comparison of the regeneration ability of the two 'systems', one being spatially more centrally and the other more peripherally located; and (vi) octopuses represents a 'simpler' animal compared with vertebrates. However, regeneration/degeneration phenomena following lesion were found to be similar to those occurring in higher vertebrates (Wallerian degeneration; Imperadore et al., 2017; Sereni and Young, 1932).

Acknowledgements

The authors are thankful for the assistance and guidance given by Dr Astrid Schauss and Dr Christian Jüngst (CECAD Imaging facility, CECAD Research Center, Cologne, Germany) for accessing the imaging facility and for the use of Leica SP8 multiphoton microscope. The authors are also grateful to Leica Microsystems (P. Romano, K. Orellana) for assistance during various phases of this work. This work benefited from the networking initiative of the COST Action FA1301 – Cephs*In*Action.

Competing interests

The authors declare no competing or financial interests.

Author contributions

Conceptualization: G.F.; Formal analysis: P.I., G.F.; Investigation: P.I., D.P., A.O., M.D., A.B.; Resources: P.I., D.P., A.O., G.F.; Writing - original draft: P.I.; Writing - review & editing: A.B., G.F.; Supervision: G.F.; Project administration: P.I.; Funding acquisition: G.F.

Funding

This work was supported by the Stazione Zoologica Anton Dohrn, Napoli (SZN), and RITMARE (Flagship Project - Ministero dell'Istruzione, dell'Università e della Ricerca & SZN) to G.F., and by the Association for Cephalopod Research - CephRes to P.I. This work also benefited from the infrastructure part of the project 'Potenziamento di una piattaforma integrata per lo studio di malattie umane di grande impatto attraverso l'uso del system phenotyping di modelli animali: Mouse e Zebrafish clinic (MouZeCLINIC)' to the SZN (PONREC PONa3_00239).

Supplementary information

Supplementary information available online at
http://jeb.biologists.org/lookup/doi/10.1242/jeb.209965.supplemental

References

Amodio, P., Andrews, P., Salemme, M., Ponte, G. and Fiorito, G. (2014). The use of artificial crabs for testing predatory behavior and health in the octopus. *Altex-Alternat. Anim. Exp.* **31**, 494-499. doi:10.14573/altex.1401282

Andrews, P. L. R., Darmaillacq, A.-S., Dennison, N., Gleadall, I. G., Hawkins, P., Messenger, J. B., Osorio, D., Smith, V. J. and Smith, J. A. (2013). The identification and management of pain, suffering and distress in cephalopods, including anaesthesia, analgesia and humane killing. *J. Exp. Mar. Biol. Ecol.* **447**, 46-64. doi:10.1016/j.jembe.2013.02.010

Birnbaum, K. D. and Alvarado, A. S. (2008). Slicing across kingdoms: regeneration in plants and animals. *Cell* **132**, 697-710. doi:10.1016/j.cell.2008.01.040

Borrelli, L. (2007). Testing the contribution of relative brain size and learning capabilities on the evolution of *Octopus vulgaris* and other cephalopods. *PhD thesis, Stazione Zoologica Anton Dohrn, Italy & Open University, UK*, 451pp.

Borrelli, L., Gherardi, F. and Fiorito, G. (2006). *A Catalogue of Body Patterning in Cephalopoda*. Napoli, Italy: Stazione Zoologica A. Dohrn; Firenze University Press.

Büschges, A., Ramirez, J.-M., Driesang, R. and Pearson, K. G. (1992). Connections of the forewing tegulae in the locust flight system and their modification following partial deafferentation. *J. Neurobiol.* **23**, 44-60. doi:10.1002/neu.480230106

Butler-Struben, H. M., Brophy, S. M., Johnson, N. A. and Crook, R. J. (2018). In vivo recording of neural and behavioral correlates of anesthesia induction, reversal, and euthanasia in cephalopod molluscs. *Front. Physiol.* **9**, 109. doi:10.3389/fphys.2018.00109

Festing, M. F. W. and Altman, D. G. (2002). Guidelines for the design and statistical analysis of experiments using laboratory animals. *ILAR J.* **43**, 244-258. doi:10.1093/ilar.43.4.244

Fiorito, G. and Scotto, P. (1992). Observational learning in *Octopus vulgaris*. *Science* **256**, 545-547. doi:10.1126/science.256.5056.545

Fiorito, G., von Planta, C. and Scotto, P. (1990). Problem solving ability of *Octopus vulgaris* Lamarck (Mollusca, Cephalopoda). *Behav. Neural Biol.* **53**, 217-230. doi:10.1016/0163-1047(90)90441-8

Fiorito, G., Affuso, A., Anderson, D. B., Basil, J., Bonnaud, L., Botta, G., Cole, A., D'Angelo, L., de Girolamo, P., Dennison, N. et al. (2014). Cephalopods in neuroscience: regulations, research and the 3Rs. *Invert. Neurosci* **14**, 13-36. doi:10.1007/s10158-013-0165-x

Fiorito, G., Affuso, A., Basil, J., Cole, A., de Girolamo, P., D'Angelo, L., Dickel, L., Gestal, C., Grasso, F., Kuba, M. et al. (2015). Guidelines for the care and welfare of cephalopods in research - a consensus based on an initiative by CephRes, FELASA and the Boyd Group. *Lab. Anim.* **49**, 1-90. doi:10.1177/0023677215580006

Fredericq, L. (1878). Recherches sur la Physiologie du poulpe commun. *Arch. Zool. Exp. Génér.* **7**, 535-583.

Gleadall, I. G. (2013). The effects of prospective anaesthetic substances on cephalopods: summary of original data and a brief review of studies over the last two decades. *J. Exp. Mar. Biol. Ecol* **447**, 23-30. doi:10.1016/j.jembe.2013.02.008

Grimaldi, A. M., Agnisola, C. and Fiorito, G. (2007). Using ultrasound to estimate brain size in the cephalopod *Octopus vulgaris* Cuvier in vivo. *Brain Res.* **1183**, 66-73. doi:10.1016/j.brainres.2007.09.032

Hooper, S. L. and Schmidt, J. (2017). Electrophysiological recording techniques. In *Neurobiology of Motor Control: Fundamental Concepts and New Directions* (ed. S. L. Hooper and A. Büschges), pp. 7-54. Hoboken, NJ, USA: Wiley-Blackwell.

Imperadore, P. (2017). Nerve regeneration in the cephalopod mollusc *Octopus vulgaris*: a journey into morphological, cellular and molecular changes including epigenetic modifications. *PhD thesis*, *Dipartimento di Biologia, Ecologia e Scienze della Terra, Università della Calabria, Italy*, 236pp.

Imperadore, P. and Fiorito, G. (2018). Cephalopod tissue regeneration: consolidating over a century of knowledge. *Front. Physiol.* **9**, 593. doi:10.3389/fphys.2018.00593

Imperadore, P., Shah, S. B., Makarenkova, H. P. and Fiorito, G. (2017). Nerve degeneration and regeneration in the cephalopod mollusc *Octopus vulgaris*: the case of the pallial nerve. *Sci. Rep.* **7**, 46564. doi:10.1038/srep46564

Imperadore, P., Uckermann, O., Galli, R., Steiner, G., Kirsch, M. and Fiorito, G. (2018). Nerve regeneration in the cephalopod mollusc *Octopus vulgaris*: label-free multiphoton microscopy as a tool for investigation. *J. R. Soc. Interface* **15**, 20170889. doi:10.1098/rsif.2017.0889

Imperadore, P., Lepore, M. G., Ponte, G., Pflüger, H.-J. and Fiorito, G. (2019). Neural pathways in the pallial nerve and arm nerve cord revealed by neurobiotin backfilling in the cephalopod mollusk *Octopus vulgaris*. *Invertebr. Neurosci.* **19**, 5. doi:10.1007/s10158-019-0225-y

Kang, H. and Lichtman, J. W. (2013). Motor axon regeneration and muscle reinnervation in young adult and aged animals. *J. Neurosci.* **33**, 19480-19491. doi:10.1523/JNEUROSCI.4067-13.2013

Maldonado, H. (1963a). The positive learning process in *Octopus vulgaris*. *Z. Vergl. Physiol.* **47**, 191-214. doi:10.1007/BF00303120

Maldonado, H. (1963b). The visual attack learning system in *Octopus vulgaris*. *J. Theor. Biol* **5**, 470-488. doi:10.1016/0022-5193(63)90090-0

Messenger, J. B. (2001). Cephalopod chromatophores: neurobiology and natural history. *Biol. Rev.* **76**, 473-528. doi:10.1017/S1464793101005772

Monsell, E. M. (1977). The Organization of the stellate ganglion: a study of synaptic architecture and amacrine neurons in octopus. *PhD thesis*, Duke University, 93pp.

Packard, A. (1963). The behaviour of *Octopus vulgaris*. *Bull. Institut Océanogr. Num. Spéc.* **1D**, 35-49.

Packard, A. (1991). Uses of nicotine to follow denervation supersensitivity in unilaterally denervated octopus in vivo. *J. Physiol.* **438**, 325-325.

Packard, A. (1995). Through the looking-glass of cephalopod colour patterns. In *Behavioural Brain Research in Naturalistic and Semi-Naturalistic Settings* (ed. E. Alleva, A. Fasolo, H.-P. Lipp, L. Nadel and L. Ricceri), pp. 105-130. Dordrecht: Kluwer Academic.

Packard, A. and Hochberg, F. G. (1977). Skin patterning in *Octopus* and other genera. *Symp. Zool. Soc. Lond.* **38**, 191-231.

Sanders, G. D. and Young, J. Z. (1974). Reappearance of specific colour patterns after nerve regeneration in *Octopus*. *Proc. R. Soc. Lond. B. Biol. Sci.* **186**, 1-11. doi:10.1098/rspb.1974.0031

Sauer, A., Driesang, R., Büschges, A. and Bässler, U. (1995). Information processing in the femur-tibia control loop of stick insects. *J. Comp. Physiol. A* **177**, 145-158. doi:10.1007/BF00225095

Sereni, E. (1929). Fenomeni fisiologici consecutivi alla sezione dei nervi nei cefalopodi. *Boll. Soc. It. Biol. Sperim* **4**, 736-740.

Sereni, E. and Young, J. Z. (1932). Nervous degeneration and regeneration in Cephalopods. *Pubbl. Staz. Zool. Napoli* **12**, 173-208.

Siegel, S. and Castellan, N. J. (1988). *Nonparametric Statistics for the Behavioral Sciences*. New York: McGraw-Hill.

Smith, J. A., Andrews, P. L. R., Hawkins, P., Louhimies, S., Ponte, G. and Dickel, L. (2013). Cephalopod research and EU Directive 2010/63/EU: requirements, impacts and ethical review. *J. Exp. Mar. Biol. Ecol.* **447**, 31-45. doi:10.1016/j.jembe.2013.02.009

Young, J. Z. (1929). Fenomeni istologici consecutivi alla sezione dei nervi nei cefalopodi. *Boll. Soc. It. Biol. Sperim.* **4**, 741-744.

Young, J. Z. (1971). *The Anatomy of the Nervous System of Octopus vulgaris*. London, UK: Oxford University Press.

Young, J. Z. (1972). The Organization of a Cephalopod Ganglion. *Philos. Trans. R. Soc. B* **263**, 409-429. doi:10.1098/rstb.1972.0005

Zar, J. H. (1999). *Biostatistical Analysis*. Upper Saddle River, NJ: Prentice Hall.

Zullo, L., Fossati, S. M., Imperadore, P. and Nödl, M.-T. (2017). Molecular determinants of Cephalopod muscles and their implication in muscle regeneration. *Front. Cell. Dev. Biol.* **5**, 53. doi:10.3389/fcell.2017.00053

Supplementary figures

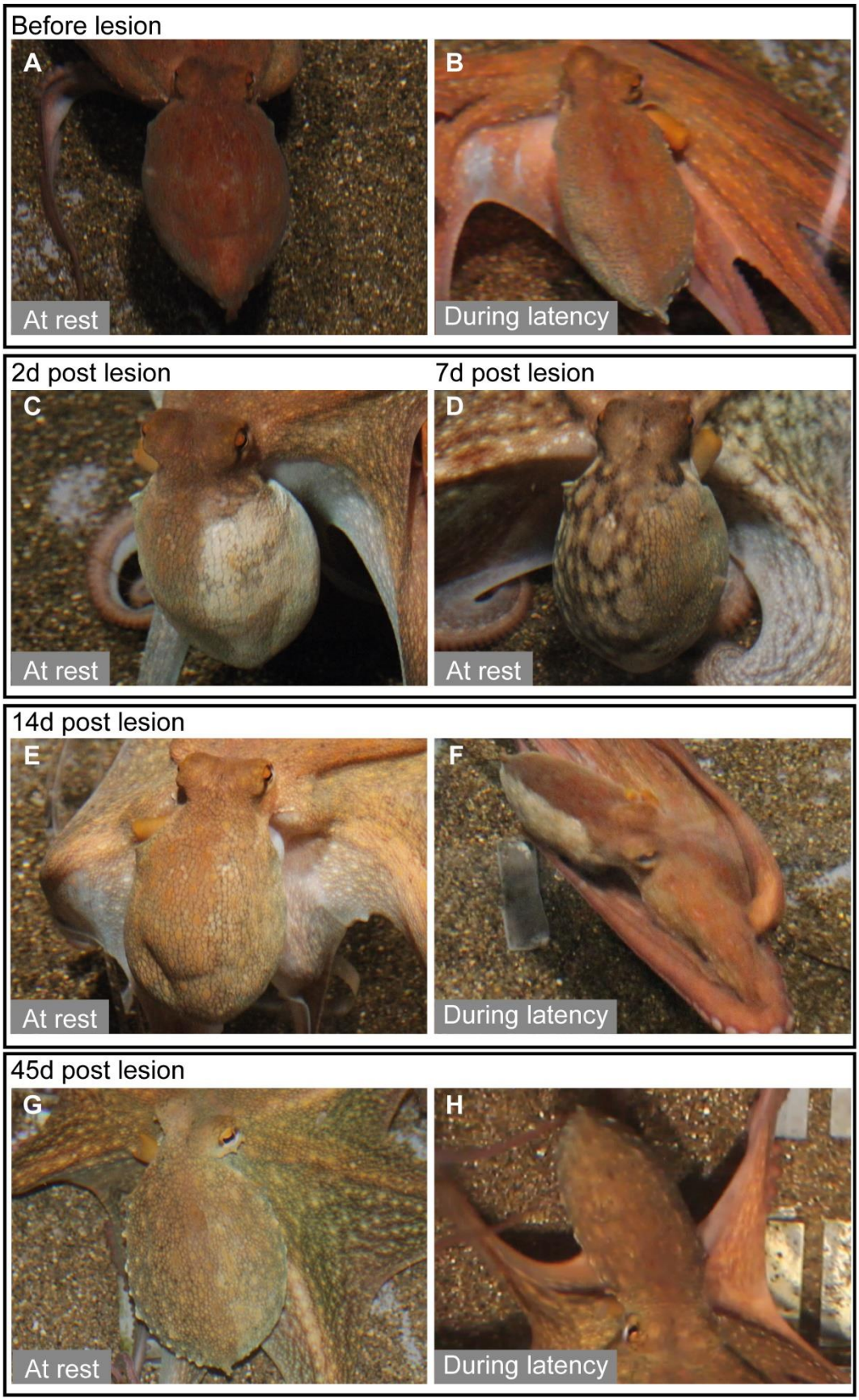

Figure S1. Skin functional recovery. Uninjured animals can tune body pattern bilaterally on the mantle (e.g. at rest in **A**) or unilaterally if necessary (e.g. during predatory performance in **B**). Two days post lesion (**C**) brown spots appear random on the denervated skin. A few days after, the whole affected skin area assumed a uniform colour (**D**) with some ability in matching contralateral side at rest (**E**). This ability is not retained during latency of attack (**F**) with the injured side becoming completely pale. Only 45 days to four months post lesion full control on skin patterning is resumed and observable both at rest and during prey attack (Unilateral effect, **G**; Uniform phase, **H**).

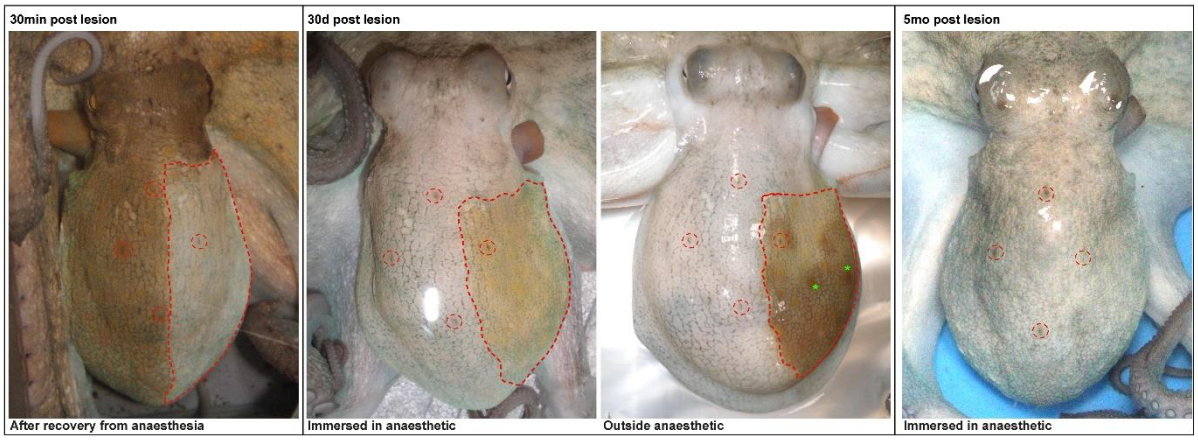

Figure S2. Effect of anaesthesia on octopus denervated skin. Soon after lesion (30 min post lesion) recovered animals show complete paling of the skin on the ipsilateral side of the lesion (denervated area is highlighted by red dotted line; red dotted circles are used to highlight the four main papillae hereby used as landmarks). 30 days (30d) post lesion the denervated skin of animals immersed in the anaesthetic gets yellowish in colour, in contrast to the rest of the body which respond to anaesthesia by paling. If only the mantle is taken out from anaesthetic solution, dark waves start propagating random on the skin (visible as dark brown spots, highlighted by green asterisks). The injured side also shows a reduction in the size of the denervated skin with time, highlighted by red dotted lines.

All these effects disappear in long denervated animals that fully recovered the lost function (e.g. five months – 5mo post lesion) with skin completely and homogeneously paling in anaesthetic solution.

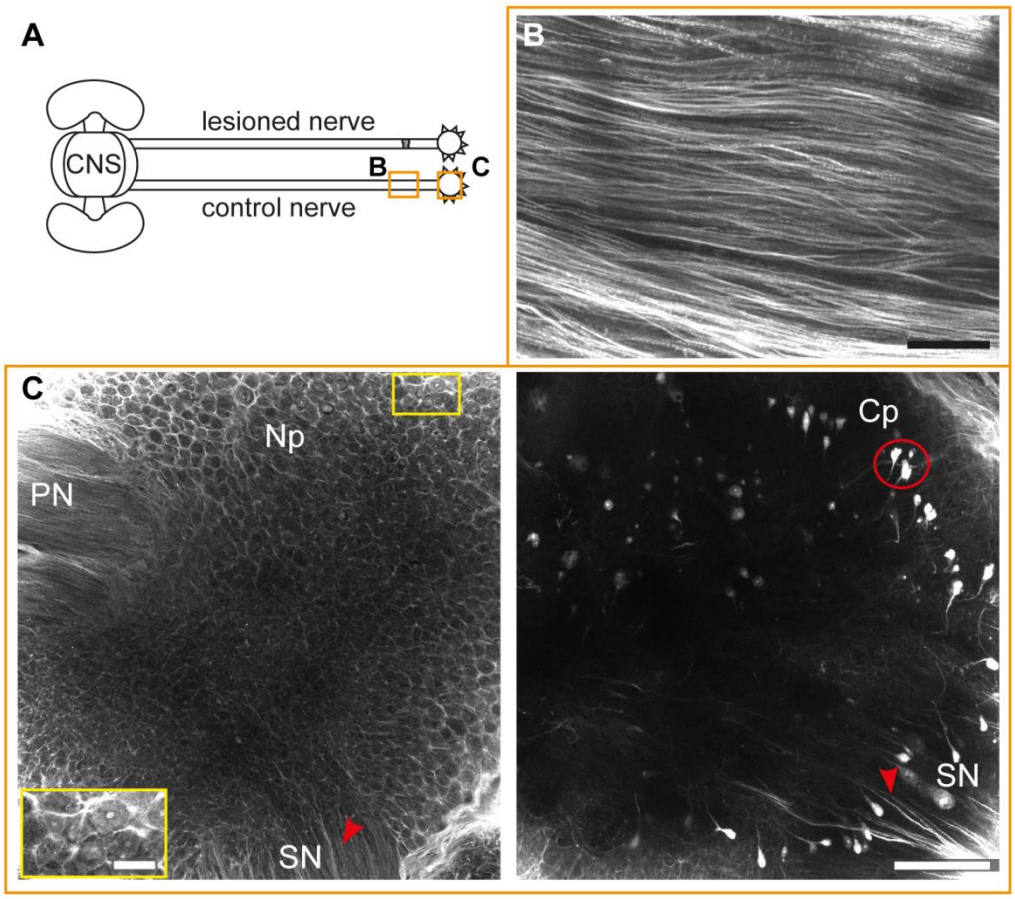

Figure S3. Backfilling of control pallial nerve. (**A**) Schematic drawing of the connections between the CNS and the periphery through the pallial nerves (PN). The orange rectangles highlight the area depicted in (**B**, **C**), corresponding to the control pallial nerve (**B**) and the control stellate ganglion (**C**). (**B**) Fibres from and to the brain are traced with Nb running inside the pallial nerve, mainly parallel to each other. (**C**, left) When reaching the stellate ganglion, some of these axons form an intricate neuropil (Np) around motoneurons (see enlargement in the yellow rectangle) and exit through the stellar nerves (SN) (red arrowheads) to innervate the chromatophores in

the skin. (**C**, right) Other fibres originate from the centripetal cells (Cp) inside the ganglion (marked by red circle).

Scale bars: (**B**) 150 μm, (**C**) 500 μm, yellow rectangle 100 μm. Abbreviations: CNS, central nervous system; Cp, centripetal cells; PN, pallial nerve; Np, neuropil; SN, stellar nerve.

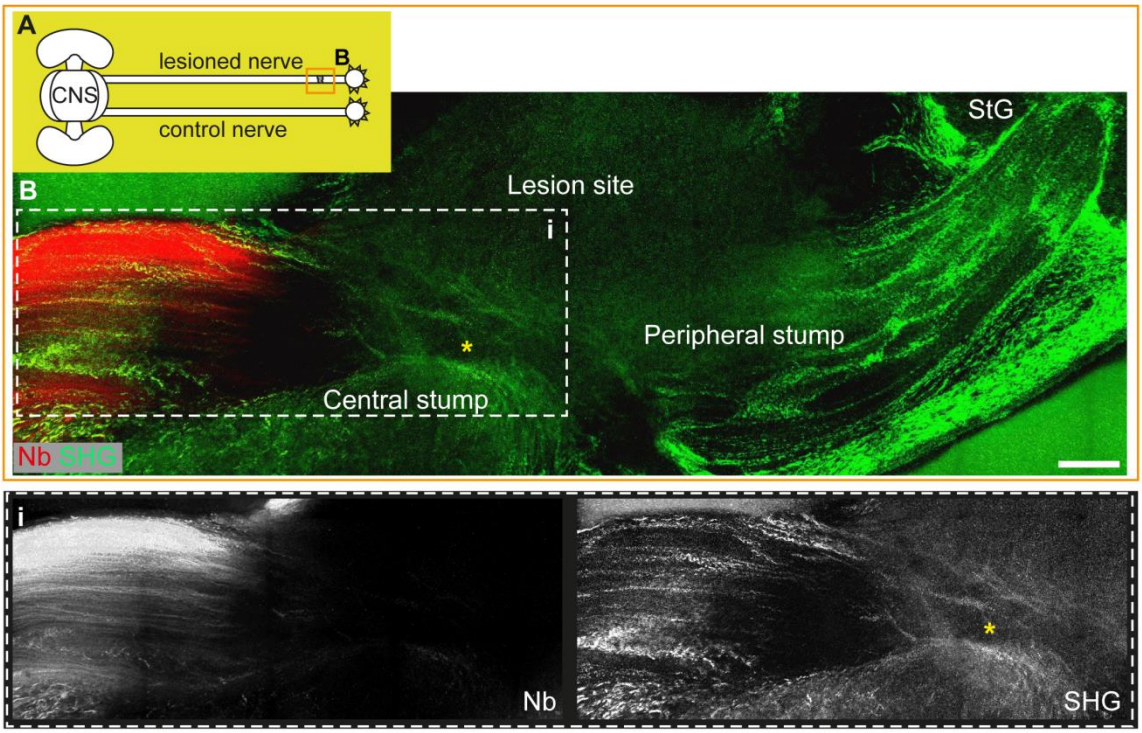

Figure S4. Backfilling of the nerve five days post lesion. (**A**) Schematic drawing of the connections between the central brain (CNS) and the periphery through the pallial nerves. The orange rectangle highlights the areas depicted in (**B**), corresponding to the lesioned pallial nerve. (**B**) Shows a nerve five days post lesion in which neurobiotin (Nb, in red in the merged image) traces fibres only in the central stump. These fibres, although regenerating, do not cross the lesion site. SHG (in green in the merged image) highlights the connective tissue enwrapping the nerve and marks up both the central and the peripheral stump. This allows identification of a spike like structure of connective tissue around the central stump bridging it to the peripheral one. The latter doesn't contain any traced neural fibre. (**Bi**) Shows a zoom-in of the central stump in (**B**) with single channels for Nb and SHG. Scale bar: 250 μm. Abbreviations: CNS, Central Nervous System; Nb, Neurobiotin; SHG, Second Harmonic Generation; StG, Stellate Ganglion.

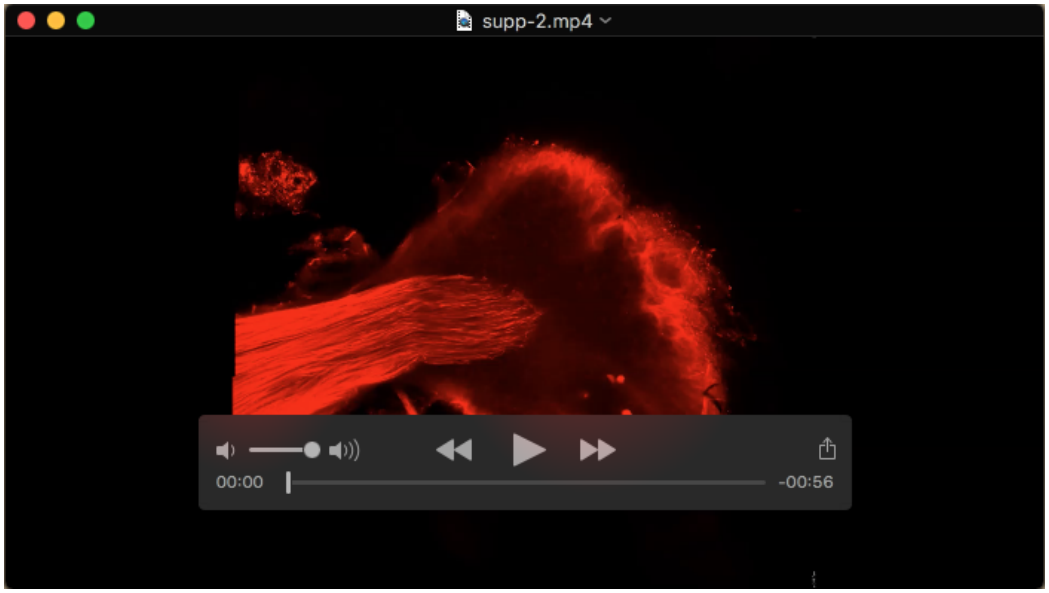

Movie 1. Backfilling of a control pallial nerve. The control pallial nerve, backfilled with neurobiotin, is visible in red. Fibres are seen to run straight in the pallial nerve and reach the stellate ganglion. These fibres take part in forming the neuropil of the ganglion. Some of them do not form synapsis in the ganglion but directly run through the stellar nerves to innervate the chromatophores or come from the periphery to reach the CNS. Other fibres stop in the ganglion, forming synapsis with the motoneurons, which then innervate respiratory muscles. In the ganglion it is also possible to observe the presence of cells, named centripetal cells, sending their axons toward the pallial nerve.

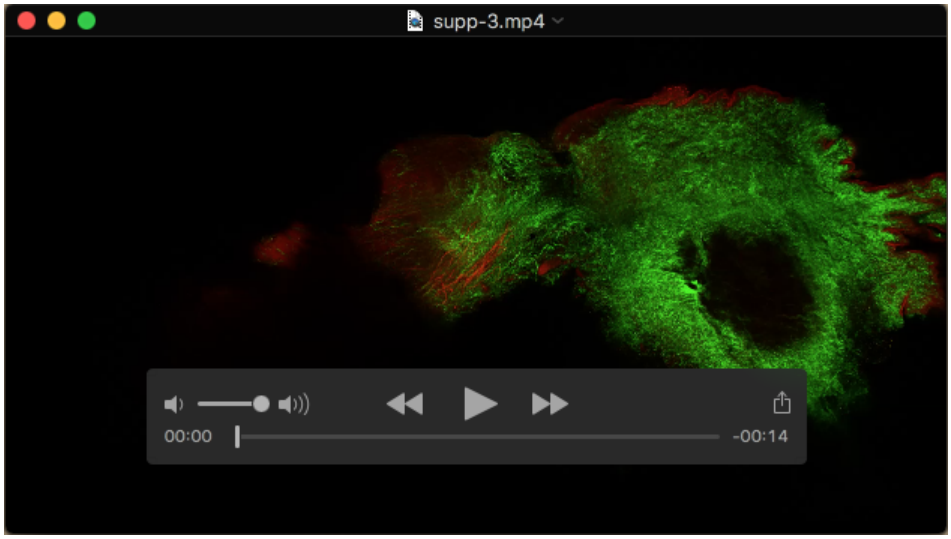

Movie 2. Backfilling of the pallial nerve 45 days post lesion. A lesioned pallial nerve, 45 days post lesion, is backfilled with neurobiotin (in red) through its central stump. SHG is used to image connective tissue. See Figure 4 for details. In the second part of the video, a zoom-in of the lesioned site is of the same nerve is shown (Nb in red, SHG in green).